

J/ψ Elliptic Flow in Pb-Pb Collisions at $\sqrt{s_{NN}} = 2.76$ TeVE. Abbas *et al.**
(ALICE Collaboration)

(Received 24 March 2013; revised manuscript received 28 July 2013; published 17 October 2013)

We report on the first measurement of inclusive J/ψ elliptic flow v_2 in heavy-ion collisions at the LHC. The measurement is performed with the ALICE detector in Pb-Pb collisions at $\sqrt{s_{NN}} = 2.76$ TeV in the rapidity range $2.5 < y < 4.0$. The dependence of the J/ψ v_2 on the collision centrality and on the J/ψ transverse momentum is studied in the range $0 \leq p_T < 10$ GeV/ c . For semicentral Pb-Pb collisions at $\sqrt{s_{NN}} = 2.76$ TeV, an indication of nonzero v_2 is observed with a largest measured value of $v_2 = 0.116 \pm 0.046(\text{stat}) \pm 0.029(\text{syst})$ for J/ψ in the transverse momentum range $2 \leq p_T < 4$ GeV/ c . The elliptic flow measurement complements the previously reported ALICE results on the inclusive J/ψ nuclear modification factor and favors the scenario of a significant fraction of J/ψ production from charm quarks in a deconfined partonic phase.

DOI: [10.1103/PhysRevLett.111.162301](https://doi.org/10.1103/PhysRevLett.111.162301)

PACS numbers: 25.75.Cj, 25.75.Ld, 25.75.Nq

Ultrarelativistic heavy-ion collisions enable the study of matter at high temperature and pressure where quantum chromodynamics predicts the existence of a deconfined state of partonic matter, the quark-gluon plasma (QGP). Heavy quarks are expected to be produced in the primary partonic scatterings and to interact with this partonic medium making them ideal probes of the QGP. Quarkonia (a heavy quark and antiquark bound state) are therefore expected to be sensitive to the properties of the strongly interacting system formed in the early stages of heavy-ion collisions [1]. According to the color-screening model [2], quarkonium states are suppressed in the medium with different dissociation probabilities for the various states. Recently, the CMS Collaboration at the Large Hadron Collider (LHC) reported about the observation of the sequential suppression in the Υ sector [3]. The ALICE Collaboration published the inclusive [4] J/ψ nuclear modification factor R_{AA} down to zero transverse momentum (p_T) at forward rapidity in Pb-Pb collisions at $\sqrt{s_{NN}} = 2.76$ TeV [5]. The R_{AA} compares the yields in Pb-Pb to those in pp collisions scaled by the number of binary nucleon-nucleon collisions. The inclusive J/ψ R_{AA} reported is larger than that measured at the SPS [6] and at RHIC [7,8] for central collisions and does not exhibit a significant centrality dependence. Complementarily, the CMS Collaboration measured the high p_T ($6.5 \leq p_T < 30$ GeV/ c) prompt J/ψ R_{AA} in the rapidity range $|y| < 2.4$ [9]. The CMS data show that high p_T J/ψ are more suppressed than low p_T J/ψ and that this suppression does exhibit a strong centrality dependence.

The low p_T J/ψ R_{AA} can be qualitatively understood with models including full [10,11] or partial [12,13] regeneration of J/ψ from deconfined charm quarks in the medium. This mechanism was first proposed by the statistical hadronization model, which assumes deconfinement and thermal equilibrium of the bulk of $c\bar{c}$ pairs to produce J/ψ at the phase boundary by statistical hadronization only [10]. Later, the transport models proposed a dynamical competition between the J/ψ suppression by the QGP and the regeneration mechanism, which enables them to also describe the J/ψ R_{AA} versus p_T [12,13]. More differential studies, like the J/ψ elliptic flow, could help to assess the assumption of charm quark thermalization in the medium.

The azimuthal distribution of particles in the transverse plane is also sensitive to the dynamics of the early stages of heavy-ion collisions. In noncentral collisions, the geometrical overlap region and, therefore, the initial matter distribution are anisotropic (almond shaped). If the matter is strongly interacting, this spatial asymmetry is converted via multiple collisions into an anisotropic momentum distribution [14]. The second coefficient of the Fourier expansion describing the final state particle azimuthal distribution with respect to the reaction plane v_2 is called elliptic flow. The reaction plane is defined by the beam axis and the impact parameter vector of the colliding nuclei.

Within the transport model scenario [12,13] observed J/ψ have two origins. First, primordial J/ψ produced in the initial hard scatterings traverse and interact with the created medium. During this process they may be dissociated. Second, J/ψ could be regenerated from deconfined charm quarks in the QGP. Primordial J/ψ emitted in plane traverse a shorter path through the medium than those emitted out of plane, resulting in a small azimuthal anisotropy for the surviving J/ψ . Regenerated J/ψ inherit the elliptic flow of the charm quarks in the QGP. If charm quarks do thermalize in the QGP, then J/ψ formed there

*Full author list given at the end of the article.

can exhibit a large elliptic flow. In the calculation by Zhao *et al.* [15], the v_2 of J/ψ at $p_T \approx 2.5$ GeV/ c is 0.02 and 0.2 for primordial and regenerated J/ψ , respectively.

At RHIC, the (preliminary) measurements by the (PHENIX) STAR Collaboration of the J/ψ v_2 in Au-Au collisions at $\sqrt{s_{NN}} = 200$ GeV [16,17] are consistent with zero albeit with large uncertainties in the p_T and centrality ranges (0–5 GeV/ c) 2–10 GeV/ c and (20%–60%) 10%–40%. In Pb-Pb collisions at the LHC, the higher energy density of the medium should favor the charm quark thermalization, and thus increase its flow. In addition, the large number of $c\bar{c}$ pairs produced should favor the formation of J/ψ by regeneration mechanisms. Both effects should lead to an increase of the v_2 of the observed J/ψ .

In this Letter, we report ALICE results on inclusive J/ψ elliptic flow in Pb-Pb collisions at $\sqrt{s_{NN}} = 2.76$ TeV at forward rapidity, measured via the $\mu^+\mu^-$ decay channel. The results are presented as a function of transverse momentum and collision centrality.

The ALICE detector is described in [18]. At forward rapidity ($2.5 < y < 4$) the production of quarkonia is measured in the muon spectrometer [19] down to $p_T = 0$. The spectrometer consists of an absorber stopping the hadrons in front of five tracking stations comprising two planes of cathode pad chambers each, with the third station inside a dipole magnet. The tracking apparatus is completed by a triggering system made of four planes of resistive plate chambers downstream of an iron wall, which absorbs secondary hadrons escaping from the front absorber and low momentum muons. Also used in this analysis are two cylindrical layers of silicon pixel detectors, to determine the location of the interaction point, and two scintillator arrays (VZERO). The VZERO counters consist of two arrays of 32 scintillator sectors each distributed in four rings covering $2.8 \leq \eta \leq 5.1$ (VZERO-A) and $-3.7 \leq \eta \leq -1.7$ (VZERO-C). All of these detectors have full azimuthal coverage. The data sample used for this analysis, collected in 2011, amounts to 17×10^6 dimuon unlike sign (MU) triggered Pb-Pb collisions and corresponds to an integrated luminosity $\mathcal{L}_{\text{int}} \approx 70 \mu\text{b}^{-1}$. The MU trigger requires a minimum bias (MB) trigger and at least a pair of opposite-sign (OS) track segments, each with a p_T above the threshold of the on-line trigger algorithm. This p_T threshold was set to provide 50% efficiency for muon tracks with $p_T = 1$ GeV/ c . The MB trigger requires a signal in both VZERO-A and VZERO-C. The beam-induced background was further reduced off-line using the VZERO and the zero degree calorimeter timing information. The contribution from electromagnetic processes was removed by requiring a minimum energy deposited in the neutron zero degree calorimeters [20]. The centrality determination is based on a fit of the VZERO amplitude distribution [21,22]. The average number of participating nucleons $\langle N_{\text{part}} \rangle$ for the centrality classes used in this

TABLE I. $\langle N_{\text{part}} \rangle$ and VZERO-A EP resolution for the centrality classes expressed in percentages of the nuclear cross section [21].

Centrality	$\langle N_{\text{part}} \rangle$	EP resolution $\pm(\text{stat}) \pm(\text{syst})$
5%–20%	283 ± 4	$0.548 \pm 0.003 \pm 0.009$
20%–40%	157 ± 3	$0.610 \pm 0.002 \pm 0.008$
40%–60%	69 ± 2	$0.451 \pm 0.003 \pm 0.008$
60%–90%	15 ± 1	$0.185 \pm 0.005 \pm 0.013$
20%–60%	113 ± 3	$0.576 \pm 0.002 \pm 0.008$

analysis (see Table I) are derived from a Glauber model calculation [21,22].

J/ψ candidates are formed by combining pairs of OS tracks reconstructed in the geometrical acceptance of the muon spectrometer. To improve the muon identification, the reconstructed tracks in the tracking chambers are required to match a track segment in the trigger system above the p_T threshold aforementioned.

The J/ψ v_2 is calculated using event plane (EP) based methods. The azimuthal angle Ψ of the second harmonic EP is used to estimate the reaction plane angle [23]. Ψ is determined from the azimuthal distribution of the VZERO amplitude. A two step flattening procedure of the EP azimuthal distribution was applied as described in [24] and [25], respectively. It results in an EP azimuthal distribution uniform to better than 2% for all centrality classes under study. The VZERO-C has a common acceptance region with the muon spectrometer. Therefore, only the VZERO-A was used for the EP determination to avoid autocorrelations. The J/ψ v_2 results were obtained determining $v_2 = \langle \cos 2(\phi - \Psi) \rangle$ versus the invariant mass ($m_{\mu\mu}$) [26], where ϕ is the OS dimuon azimuthal angle. The resulting $v_2(m_{\mu\mu})$ distribution is fitted using

$$v_2(m_{\mu\mu}) = v_2^{\text{sig}} \alpha(m_{\mu\mu}) + v_2^{\text{bkg}}(m_{\mu\mu})[1 - \alpha(m_{\mu\mu})], \quad (1)$$

where v_2^{sig} and v_2^{bkg} correspond to the v_2 of the J/ψ signal and of the background, respectively [see Fig. 1(b)]. v_2^{bkg} was parametrized using a second order polynomial. Here, $\alpha(m_{\mu\mu}) = S/(S+B)$ is the ratio of the signal over the sum of the signal plus background of the $m_{\mu\mu}$ distributions. It is extracted from fits to the OS invariant mass distribution [see Fig. 1(a)] in each p_T and centrality class. The J/ψ line shape was described with a Crystal Ball (CB) function and the underlying continuum with either a third order polynomial or a Gaussian with a width linearly varying with mass. The CB function connects a Gaussian core with a power-law tail [27] at low mass to account for energy loss fluctuations and radiative decays. An extended CB function with an additional power-law tail at high mass, to account for alignment and calibration biases, was also used. The combination of several CB and underlying continuum parametrizations described before were tested to assess the signal and the related systematic

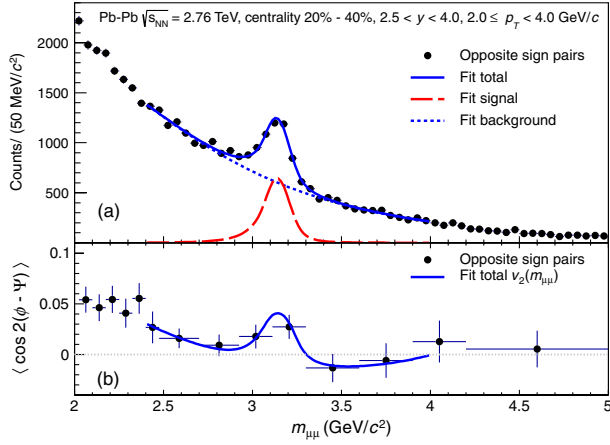


FIG. 1 (color online). Invariant mass distribution (a) and $\langle \cos 2(\phi - \Psi) \rangle$ as a function of $m_{\mu\mu}$ (b) of OS dimuons with $2 \leq p_T < 4$ GeV/c and $2.5 < y < 4$ in semicentral (20%–40%) Pb-Pb collisions.

uncertainties. The J/ψ v_2 and its statistical uncertainty in each p_T and centrality class were determined as the average of the v_2^{sig} obtained by fitting $v_2(m_{\mu\mu})$ using Eq. (1) with the various $\alpha(m_{\mu\mu})$, while the corresponding systematic uncertainties were defined as the rms of these results. Figure 1 shows typical fits of the OS invariant mass distribution [1(a)] and of the $\langle \cos 2(\phi - \Psi) \rangle$ as a function of $m_{\mu\mu}$ [1(b)] in the 20%–40% centrality class. The procedure above was repeated using either a first order polynomial or its inverse as v_2^{bkg} parametrization. The largest deviation of the results obtained with the three different v_2^{bkg} parametrizations was conservatively adopted as the systematic uncertainty related to the unknown shape of the $v_2^{\text{bkg}}(m_{\mu\mu})$. This turns out to often be the dominant source of systematic uncertainties with the uncertainty from the signal extraction being the second one. It was checked that different choices of invariant mass binnings yield v_2 values that are consistent within uncertainties. A similar method was used to extract the uncorrected (for detector acceptance and efficiency) average transverse momentum ($\langle p_T \rangle^{\text{uncor}}$) of the reconstructed J/ψ in each centrality and p_T class. The $\langle p_T \rangle^{\text{uncor}}$ is used to locate the data points when plotted as a function of p_T . Consistent v_2 values were obtained using an alternative method [23] in which the J/ψ raw yield is extracted, as described before, in bins of $(\phi - \Psi)$ and v_2 is evaluated by fitting the data with the function $(dN/d(\phi - \Psi)) = A[1 + 2v_2 \cos 2(\phi - \Psi)]$, where A is a normalization constant. As an additional check the first analysis procedure [26] was also applied to the same-sign (SS) dimuons. As expected, no J/ψ signal is seen in either the invariant mass distribution or the $\langle \cos 2(\phi - \Psi) \rangle$ as a function of $m_{\mu\mu}$ of SS dimuons. In both cases the SS dimuons exhibit the same trend as the continuum of the OS dimuons.

The finite resolution in the EP determination smears out the azimuthal distributions and lowers the value of the measured anisotropy [23]. The VZERO-A EP resolution as a function of the centrality was determined using MB events and the 3 subevent method [23]. To estimate the systematic uncertainty from the EP determination two sets of 3 subevents were used: first, VZERO-A, VZERO-C, and the time projection chamber (TPC), with pseudorapidity gaps $\Delta\eta_{\text{VZERO-A-TPC}} = 1.9$, $\Delta\eta_{\text{VZERO-A-VZERO-C}} = 4.5$, and $\Delta\eta_{\text{TPC-VZERO-C}} = 0.8$; second, VZERO-A, ring 0 of VZERO-C, and VZERO-C 3rd ring, with pseudorapidity gaps $\Delta\eta_{\text{VZERO-A-VZERO-C0}} = 6.0$, $\Delta\eta_{\text{VZERO-C0-VZERO-C3}} = 1.0$, and $\Delta\eta_{\text{VZERO-A-VZERO-C3}} = 4.5$. The differences between the EP resolution for VZERO-A obtained from these two sets of subevents are taken as systematic uncertainties. Since v_2 is measured here in a wide centrality class, the resolution must reflect the distribution of events with a J/ψ within the class. Therefore, the EP resolution for each wide class was calculated as the average of the values obtained in finer centrality classes weighted by the number of reconstructed J/ψ . Table I shows the corresponding resolution for each centrality class which is applied to the results reported in this Letter.

The J/ψ reconstruction efficiency depends on the detector occupancy, which could bias the v_2 measurement. This effect was evaluated by embedding azimuthally isotropic simulated $J/\psi \rightarrow \mu^+ \mu^-$ decays into real events. The measured v_2 of those embedded J/ψ does not deviate from zero by more than 0.015 in the centrality and p_T classes considered. This value is used as a conservative systematic uncertainty on all measured v_2 values.

Figure 2 shows the p_T dependence of the inclusive J/ψ v_2 for semicentral (20%–40%) Pb-Pb collisions at $\sqrt{s_{NN}} = 2.76$ TeV. The vertical bars show the statistical uncertainties while the boxes indicate the point-to-point uncorrelated systematic uncertainties, which include those from

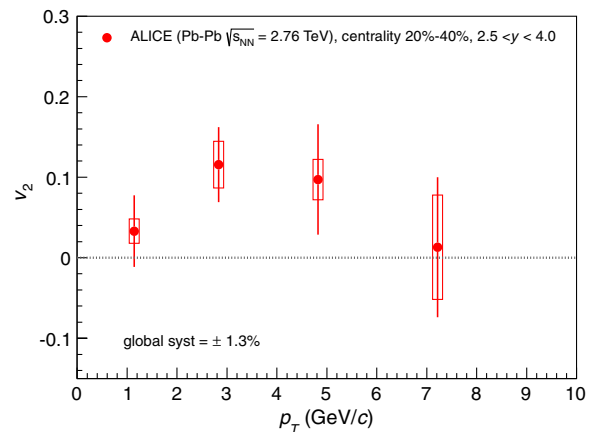


FIG. 2 (color online). Inclusive J/ψ $v_2(p_T)$ for semicentral (20%–40%) Pb-Pb collisions at $\sqrt{s_{NN}} = 2.76$ TeV (see text for details on uncertainties). The used p_T ranges are 0–2, 2–4, 4–6, and 6–10 GeV/c.

the signal extraction, the v_2^{bkg} shape, and the reconstruction efficiency. The global correlated relative systematic uncertainty on the EP resolution is 1.3%. A nonzero v_2 is observed in the intermediate p_T range $2 \leq p_T < 6$ GeV/c. Including statistical and systematic uncertainties the combined significance of a nonzero v_2 in this p_T range is 2.7σ . At lower and higher p_T the inclusive J/ψ v_2 is compatible with zero within uncertainties.

To study the centrality dependence of the v_2 we select J/ψ with $1.5 \leq p_T < 10$ GeV/c. Indeed, below 1.5 GeV/c the v_2 of the J/ψ is expected to be small [15] and the signal to background ratio is also low. Since the initial spatial anisotropy for head-on collisions is small, the expected v_2 is also small. In addition, for the 0%–5% centrality range the VZERO-A EP resolution is quite low and has higher systematic uncertainties. Therefore, the 0%–5% centrality range was excluded. Figure 3(a) shows v_2 for inclusive J/ψ with $1.5 \leq p_T < 10$ GeV/c as a function of $\langle N_{\text{part}} \rangle$ in Pb-Pb collisions at $\sqrt{s_{NN}} = 2.76$ TeV. Here, the point-to-point uncorrelated systematic uncertainties (boxes) also include, in addition to those discussed above, the uncertainty from the EP resolution determination. The measured v_2 depends on the p_T distribution of the reconstructed J/ψ , which could vary with the collision centrality. Therefore, $\langle p_T \rangle^{\text{uncor}}$ of the reconstructed J/ψ is also shown in Fig. 3(b). The error bar indicates the statistical uncertainties while the boxes show the systematic uncertainties due to the J/ψ signal extraction. For the most central collisions, 5%–20% and 20%–40%, the inclusive J/ψ v_2 for $1.5 \leq p_T < 10$ GeV/c are $0.101 \pm 0.044(\text{stat}) \pm 0.032(\text{syst})$ and $0.116 \pm 0.045(\text{stat}) \pm 0.041(\text{syst})$, respectively. The combined significance of a nonzero v_2 is 2.9σ . For more peripheral Pb-Pb collisions, the v_2 is consistent with zero within uncertainties. Although there is a small variation

with centrality, the $\langle p_T \rangle^{\text{uncor}}$ stays in the range 3.0–3.3 GeV/c, indicating that the bulk of the reconstructed J/ψ are in the same p_T range for all centralities. Thus, the observed centrality dependence of the v_2 for inclusive J/ψ with $1.5 \leq p_T < 10$ GeV/c does not result from any bias in the sampled p_T distributions. For J/ψ with $p_T < 1.5$ GeV/c (not shown), the v_2 is compatible with zero within 1 standard deviation for the four centrality classes. The $\langle p_T \rangle^{\text{uncor}}$ ranges from about 0.75 to 0.9 GeV/c.

To allow a direct comparison with current model calculations, the inclusive J/ψ $v_2(p_T)$ was also calculated in a broader centrality range, namely, 20%–60%, and it is shown in Fig. 4. In this broader centrality range, the measured v_2 signal in the p_T range 2–4 GeV/c deviates from zero by 2σ . The same trend of $v_2(p_T)$ is observed in the 20%–60% and in the 20%–40% centrality classes. This trend seems qualitatively different from that of the STAR measurement [17] at lower collision energy, which is compatible with zero for $p_T \geq 2$ GeV/c albeit in somewhat different (10%–40% and 0%–80%) centrality ranges. Also shown in Fig. 4 are two transport model calculations that include a J/ψ regeneration component from deconfined charm quarks in the medium [15,28]. In both models about 30% of the measured J/ψ in the 20%–60% centrality range are regenerated. First, thermalized charm quarks in the medium transfer a significant elliptic flow to regenerated J/ψ . Second, primordial J/ψ emitted out of plane traverse a longer path through the medium than those emitted in plane, resulting in a small apparent v_2 . The predicted maximum v_2 at $p_T \sim 2.5$ GeV/c results from an interplay between the regeneration component, dominant at lower p_T , and the primordial J/ψ component which takes over at higher p_T . The first model [28] is shown for the hypothesis of thermalization (full line) and

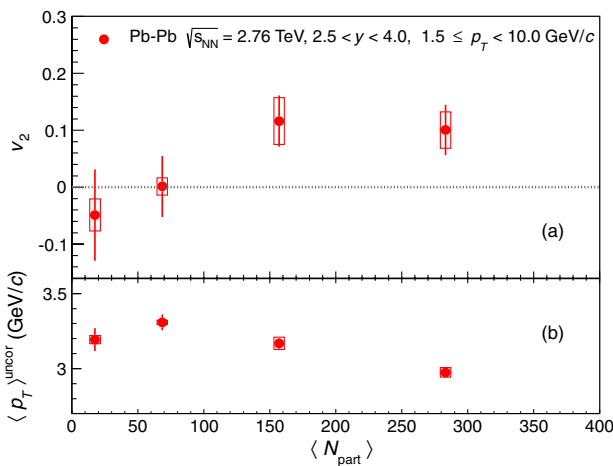


FIG. 3 (color online). v_2 (a) and $\langle p_T \rangle^{\text{uncor}}$ (b) of inclusive J/ψ with $1.5 \leq p_T < 10$ GeV/c as a function of $\langle N_{\text{part}} \rangle$ in Pb-Pb collisions at $\sqrt{s_{NN}} = 2.76$ TeV (see text for details on uncertainties).

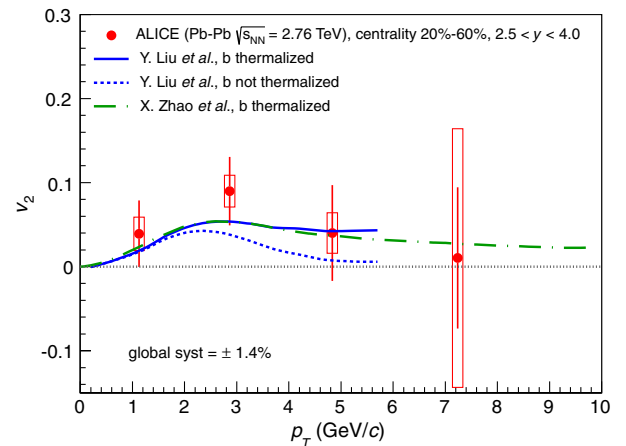


FIG. 4 (color online). Inclusive J/ψ $v_2(p_T)$ for noncentral (20%–60%) Pb-Pb collisions at $\sqrt{s_{NN}} = 2.76$ TeV (see text for details on uncertainties). The used p_T ranges are 0–2, 2–4, 4–6, and 6–10 GeV/c. Calculations from two transport models [15,28] are also shown (see text for details).

nonthermalization (dashed line) of b quarks. The LHCb Collaboration measured the fraction of J/ψ from B hadron decays in pp collisions at $\sqrt{s} = 2.76$ and 7 TeV [29,30] in the rapidity acceptance used for this measurement. At 7 TeV this fraction increases from 7% at $p_T \sim 0$ to 15% at $p_T \sim 7$ GeV/ c , while at 2.76 TeV it is about 7% for $p_T < 12$ GeV/ c . In Pb-Pb collisions this fraction could increase up to 11% if the B hadron $R_{AA} = 1$. If b quarks do thermalize, then their elliptic flow will be transferred to B mesons at hadronization and to the J/ψ at the B meson decay. In the second model [15] (dash-dotted line) only the case assuming b quark thermalization is shown. Both models qualitatively describe the p_T dependence of the v_2 and the R_{AA} of inclusive J/ψ [5].

In summary, we reported the ALICE measurement of inclusive J/ψ elliptic flow in the range $0 \leq p_T < 10$ GeV/ c at forward rapidity in Pb-Pb collisions at $\sqrt{s_{NN}} = 2.76$ TeV. For semicentral collisions indications of a nonzero J/ψ v_2 are observed in the intermediate p_T range. This measurement complements the results on the J/ψ R_{AA} , where a smaller suppression was seen at low p_T at the LHC compared to RHIC. Both results seem in agreement with the global picture in which a significant fraction of the observed J/ψ is produced from deconfined charm quarks in the QGP phase.

The ALICE Collaboration would like to thank all its engineers and technicians for their invaluable contributions to the construction of the experiment and the CERN accelerator teams for the outstanding performance of the LHC complex. The ALICE Collaboration acknowledges the following funding agencies for their support in building and running the ALICE detector: State Committee of Science, World Federation of Scientists (WFS) and Swiss Fonds Kidagan, Armenia, Conselho Nacional de Desenvolvimento Científico e Tecnológico (CNPq), Financiadora de Estudos e Projetos (FINEP), Fundação de Amparo à Pesquisa do Estado de São Paulo (FAPESP); National Natural Science Foundation of China (NSFC), the Chinese Ministry of Education (CMOE), and the Ministry of Science and Technology of China (MSTC); Ministry of Education and Youth of the Czech Republic; Danish Natural Science Research Council, the Carlsberg Foundation, and the Danish National Research Foundation; The European Research Council under the European Community's Seventh Framework Programme; Helsinki Institute of Physics and the Academy of Finland; French CNRS-IN2P3, the "Region Pays de Loire," "Region Alsace," "Region Auvergne," and CEA, France; German BMBF and the Helmholtz Association; General Secretariat for Research and Technology, Ministry of Development, Greece; Hungarian OTKA and National Office for Research and Technology (NKTH); Department of Atomic Energy and Department of Science and Technology of the Government of India; Istituto Nazionale di Fisica Nucleare (INFN) and

Centro Fermi-Museo Storico della Fisica e Centro Studi e Ricerche "Enrico Fermi," Italy; MEXT Grant-in-Aid for Specially Promoted Research, Japan; Joint Institute for Nuclear Research, Dubna; National Research Foundation of Korea (NRF); CONACYT, DGAPA, México, ALFA-EC, and the EPLANET Program (European Particle Physics Latin American Network); Stichting voor Fundamenteel Onderzoek der Materie (FOM) and the Nederlandse Organisatie voor Wetenschappelijk Onderzoek (NWO), Netherlands; Research Council of Norway (NFR); Polish Ministry of Science and Higher Education; National Authority for Scientific Research-NASR (Autoritatea Națională pentru Cercetare Științifică-ANCS); Ministry of Education and Science of Russian Federation, Russian Academy of Sciences, Russian Federal Agency of Atomic Energy, Russian Federal Agency for Science and Innovations, and The Russian Foundation for Basic Research; Ministry of Education of Slovakia; Department of Science and Technology, South Africa; CIEMAT, EELA, Ministerio de Economía y Competitividad (MINECO) of Spain, Xunta de Galicia (Consellería de Educación), CEADEN, Cubaenergía, Cuba, and IAEA (International Atomic Energy Agency); Swedish Research Council (VR) and Knut & Alice Wallenberg Foundation (KAW); Ukraine Ministry of Education and Science; United Kingdom Science and Technology Facilities Council (STFC); U.S. Department of Energy, U.S. National Science Foundation, the State of Texas, and the State of Ohio.

-
- [1] M. Bedjidian, D. Blaschke, G. T. Bodwin, N. Carrer, B. Cole *et al.*, [arXiv:hep-ph/0311048](https://arxiv.org/abs/hep-ph/0311048).
 - [2] T. Matsui and H. Satz, *Phys. Lett. B* **178**, 416 (1986).
 - [3] S. Chatrchyan *et al.* (CMS Collaboration), *Phys. Rev. Lett.* **109**, 222301 (2012).
 - [4] Inclusive J/ψ include prompt J/ψ (direct and decays from higher mass charmonium states) and nonprompt J/ψ (feed-down from b -hadron decays).
 - [5] B. Abelev *et al.* (ALICE Collaboration), *Phys. Rev. Lett.* **109**, 072301 (2012).
 - [6] B. Alessandro *et al.* (NA50 Collaboration), *Eur. Phys. J. C* **39**, 335 (2005).
 - [7] A. Adare *et al.* (PHENIX Collaboration), *Phys. Rev. Lett.* **98**, 232301 (2007).
 - [8] A. Adare *et al.* (PHENIX Collaboration), *Phys. Rev. C* **84**, 054912 (2011).
 - [9] S. Chatrchyan *et al.* (CMS Collaboration), *J. High Energy Phys.* **05** (2012) 063.
 - [10] P. Braun-Munzinger and J. Stachel, *Phys. Lett. B* **490**, 196 (2000).
 - [11] A. Andronic, P. Braun-Munzinger, K. Redlich, and J. Stachel, *J. Phys. G* **38**, 124081 (2011).
 - [12] X. Zhao and R. Rapp, *Nucl. Phys. A* **859**, 114 (2011).
 - [13] Y.-P. Liu, Z. Qu, N. Xu, and P.-F. Zhuang, *Phys. Lett. B* **678**, 72 (2009).
 - [14] J.-Y. Ollitrault, *Phys. Rev. D* **46**, 229 (1992).

- [15] X. Zhao, A. Emerick, and R. Rapp, *Nucl. Phys.* **A904–A905**, 611c (2013).
- [16] C. Silvestre for the PHENIX Collaboration, *J. Phys. G* **35**, 104136 (2008).
- [17] L. Adamczyk *et al.* (STAR Collaboration), *Phys. Rev. Lett.* **111**, 052301 (2013).
- [18] K. Aamodt *et al.* (ALICE Collaboration), *JINST* **3**, S08002 (2008).
- [19] In the ALICE reference frame, the muon spectrometer covers a negative η range and consequently a negative y range. We have chosen to present our results with a positive y notation.
- [20] B. Abelev *et al.* (ALICE Collaboration), *Phys. Rev. Lett.* **109**, 252302 (2012).
- [21] K. Aamodt *et al.* (ALICE Collaboration), *Phys. Rev. Lett.* **106**, 032301 (2011).
- [22] B. Abelev *et al.* (ALICE Collaboration), [arXiv:1301.4361](https://arxiv.org/abs/1301.4361).
- [23] A.M. Poskanzer and S.A. Voloshin, *Phys. Rev. C* **58**, 1671 (1998).
- [24] I. Selyuzhenkov and S. Voloshin, *Phys. Rev. C* **77**, 034904 (2008).
- [25] J. Barrette *et al.* (E877 Collaboration), *Phys. Rev. C* **56**, 3254 (1997).
- [26] N. Borghini and J. Y. Ollitrault, *Phys. Rev. C* **70**, 064905 (2004).
- [27] J.E. Gaiser, Ph.D. thesis, Stanford University, 1982 [SLAC Report No. SLAC-R-255, appendix F].
- [28] Y. Liu, N. Xu, and P. Zhuang, *Nucl. Phys.* **A834**, 317c (2010); (private communication).
- [29] R. Aaij *et al.* (LHCb Collaboration), *J. High Energy Phys.* **02** (2013) 041.
- [30] R. Aaij *et al.* (LHCb Collaboration), *Eur. Phys. J. C* **71**, 1645 (2011).

E. Abbas,¹ B. Abelev,² J. Adam,³ D. Adamová,⁴ A. M. Adare,⁵ M. M. Aggarwal,⁶ G. Aglieri Rinella,⁷ M. Agnello,^{8,9} A. G. Agocs,¹⁰ A. Agostinelli,¹¹ Z. Ahammed,¹² N. Ahmad,¹³ A. Ahmad Masoodi,¹³ S. A. Ahn,¹⁴ S. U. Ahn,¹⁴ I. Aimo,^{15,8,9} M. Ajaz,¹⁶ A. Akindinov,¹⁷ D. Aleksandrov,¹⁸ B. Alessandro,⁸ A. Alici,^{19,20} A. Alkin,²¹ E. Almaráz Aviña,²² J. Alme,²³ T. Alt,²⁴ V. Altini,²⁵ S. Altinpinar,²⁶ I. Altsybeev,²⁷ C. Andrei,²⁸ A. Andronic,²⁹ V. Anguelov,³⁰ J. Anielski,³¹ C. Anson,³² T. Antičić,³³ F. Antinori,³⁴ P. Antonioli,¹⁹ L. Aphecetche,³⁵ H. Appelshäuser,³⁶ N. Arbor,³⁷ S. Arcelli,¹¹ A. Arend,³⁶ N. Armesto,³⁸ R. Arnaldi,⁸ T. Aronsson,⁵ I. C. Arsene,²⁹ M. Arslanok,³⁶ A. Asryan,²⁷ A. Augustinus,⁷ R. Averbeck,²⁹ T. C. Awes,³⁹ J. Äystö,⁴⁰ M. D. Azmi,^{13,41} M. Bach,²⁴ A. Badalà,⁴² Y. W. Baek,^{43,44} R. Bailhache,³⁶ R. Bala,^{45,8} A. Baldisseri,⁴⁶ F. Baltasar Dos Santos Pedrosa,⁷ J. Bán,⁴⁷ R. C. Baral,⁴⁸ R. Barbera,⁴⁹ F. Barile,²⁵ G. G. Barnaföldi,¹⁰ L. S. Barnby,⁵⁰ V. Barret,⁴³ J. Bartke,⁵¹ M. Basile,¹¹ N. Bastid,⁴³ S. Basu,¹² B. Bathen,³¹ G. Batigne,³⁵ B. Batyunya,⁵² P. C. Batzing,⁵³ C. Baumann,³⁶ I. G. Bearden,⁵⁴ H. Beck,³⁶ N. K. Behera,⁵⁵ I. Belikov,⁵⁶ F. Bellini,¹¹ R. Bellwied,⁵⁷ E. Belmont-Moreno,²² G. Bencedi,¹⁰ S. Beole,¹⁵ I. Berceanu,²⁸ A. Bercuci,²⁸ Y. Berdnikov,⁵⁸ D. Berenyi,¹⁰ A. A. E. Bergognon,³⁵ R. A. Bertens,⁵⁹ D. Berzano,^{15,8} L. Betev,⁷ A. Bhasin,⁴⁵ A. K. Bhati,⁶ J. Bhom,⁶⁰ N. Bianchi,⁶¹ L. Bianchi,¹⁵ C. Bianchin,⁵⁹ J. Bielčik,³ J. Bielčíková,⁴ A. Bilandzic,⁵⁴ S. Bjelogrić,⁵⁹ F. Blanco,⁵⁷ F. Blanco,⁶² D. Blau,¹⁸ C. Blume,³⁶ M. Boccioni,⁷ S. Böttger,⁶³ A. Bogdanov,⁶⁴ H. Bøggild,⁵⁴ M. Bogolyubsky,⁶⁵ L. Boldizsár,¹⁰ M. Bombara,⁶⁶ J. Book,³⁶ H. Borel,⁴⁶ A. Borissov,⁶⁷ F. Bossú,⁴¹ M. Botje,⁶⁸ E. Botta,¹⁵ E. Braidot,⁶⁹ P. Braun-Munzinger,²⁹ M. Bregant,³⁵ T. Breitner,⁶³ T. A. Broker,³⁶ T. A. Browning,⁷⁰ M. Broz,⁷¹ R. Brun,⁷ E. Bruna,^{15,8} G. E. Bruno,²⁵ D. Budnikov,⁷² H. Buesching,³⁶ S. Bufalino,^{15,8} P. Buncic,⁷ O. Busch,³⁰ Z. Buthelezi,⁴¹ D. Caffarri,^{73,34} X. Cai,⁷⁴ H. Caines,⁵ E. Calvo Villar,⁷⁵ P. Camerini,⁷⁶ V. Canoa Roman,⁷⁷ G. Cara Romeo,¹⁹ W. Carena,⁷ F. Carena,⁷ N. Carlin Filho,⁷⁸ F. Carminati,⁷ A. Casanova Díaz,⁶¹ J. Castillo Castellanos,⁴⁶ J. F. Castillo Hernandez,²⁹ E. A. R. Casula,⁷⁹ V. Catanescu,²⁸ C. Cavicchioli,⁷ C. Ceballos Sanchez,⁸⁰ J. Cepila,³ P. Cerello,⁸ B. Chang,^{40,81} S. Chapeland,⁷ J. L. Charvet,⁴⁶ S. Chattopadhyay,⁸² S. Chattopadhyay,¹² M. Cherney,⁸³ C. Cheshkov,^{7,84} B. Cheynis,⁸⁴ V. Chibante Barroso,⁷ D. D. Chinellato,⁵⁷ P. Chochula,⁷ M. Chojnacki,⁵⁴ S. Choudhury,¹² P. Christakoglou,⁶⁸ C. H. Christensen,⁵⁴ P. Christiansen,⁸⁵ T. Chujo,⁶⁰ S. U. Chung,⁸⁶ C. Cicalo,⁸⁷ L. Cifarelli,^{11,20} F. Cindolo,¹⁹ J. Cleymans,⁴¹ F. Colamaria,²⁵ D. Colella,²⁵ A. Collu,⁷⁹ G. Conesa Balbastre,³⁷ Z. Conesa del Valle,^{7,88} M. E. Connors,⁵ G. Contin,⁷⁶ J. G. Contreras,⁷⁷ T. M. Cormier,⁶⁷ Y. Corrales Morales,¹⁵ P. Cortese,⁸⁹ I. Cortés Maldonado,⁹⁰ M. R. Cosentino,⁶⁹ F. Costa,⁷ M. E. Cotallo,⁶² E. Crescio,⁷⁷ P. Crochet,⁴³ E. Cruz Alaniz,²² R. Cruz Albino,⁷⁷ E. Cuautele,⁹¹ L. Cunqueiro,⁶¹ A. Dainese,^{73,34} R. Dang,⁷⁴ A. Danu,⁹² D. Das,⁸² K. Das,⁸² S. Das,⁹³ I. Das,⁸⁸ A. Dash,⁹⁴ S. Dash,⁵⁵ S. De,¹² G. O. V. de Barros,⁷⁸ A. De Caro,^{95,20} G. de Cataldo,⁹⁶ J. de Cuveland,²⁴ A. De Falco,⁹⁷ D. De Gruttola,^{95,20} H. Delagrange,³⁵ A. Deloff,⁹⁷ N. De Marco,⁸ E. Dénes,¹⁰ S. De Pasquale,⁹⁵ A. Deppman,⁷⁸ G. D'Erasmus,²⁵ R. de Rooij,⁵⁹ M. A. Diaz Corchero,⁶² D. Di Bari,²⁵ T. Dietel,³¹ C. Di Giglio,²⁵ S. Di Liberto,⁹⁸ A. Di Mauro,⁷ P. Di Nezza,⁶¹ R. Divià,⁷ Ø. Djuvsland,²⁶ A. Dobrin,^{67,85,59} T. Dobrowolski,⁹⁷ B. Dönigus,²⁹ O. Dordic,⁵³ O. Driga,³⁵ A. K. Dubey,¹² A. Dubla,⁵⁹ L. Ducroux,⁸⁴ P. Dupieux,⁴³ A. K. Dutta Majumdar,⁸² D. Elia,⁹⁶ D. Emschermann,³¹ H. Engel,⁶³ B. Erazmus,^{7,35} H. A. Erdal,²³ D. Eschweiler,²⁴ B. Espagnon,⁸⁸ M. Estienne,³⁵ S. Esumi,⁶⁰ D. Evans,⁵⁰ S. Evdokimov,⁶⁵ G. Eyyubova,⁵³ D. Fabris,^{73,34} J. Faivre,³⁷ D. Falchieri,¹¹ A. Fantoni,⁶¹ M. Fasel,³⁰ D. Fehlker,²⁶ L. Feldkamp,³¹ D. Felea,⁹² A. Feliciello,⁸ B. Fenton-Olsen,⁶⁹ G. Feofilov,²⁷

A. Fernández Téllez,⁹⁰ A. Ferretti,¹⁵ A. Festanti,⁷³ J. Figiel,⁵¹ M. A. S. Figueredo,⁷⁸ S. Filchagin,⁷² D. Finogeev,⁹⁹ F. M. Fionda,²⁵ E. M. Fiore,²⁵ E. Floratos,¹⁰⁰ M. Floris,⁷ S. Foertsch,⁴¹ P. Foka,²⁹ S. Fokin,¹⁸ E. Fragiaco,¹⁰¹ A. Francescon,^{7,73} U. Frankenfeld,²⁹ U. Fuchs,⁷ C. Furget,³⁷ M. Fusco Girard,⁹⁵ J. J. Gaardhøje,⁵⁴ M. Gagliardi,¹⁵ A. Gago,⁷⁵ M. Gallio,¹⁵ D. R. Gangadharan,³² P. Ganoti,³⁹ C. Garabatos,²⁹ E. Garcia-Solis,¹⁰² C. Gargiulo,⁷ I. Garishvili,² J. Gerhard,²⁴ M. Germain,³⁵ C. Geuna,⁴⁶ A. Gheata,⁷ M. Gheata,^{92,7} B. Ghidini,²⁵ P. Ghosh,¹² P. Gianotti,⁶¹ M. R. Girard,¹⁰³ P. Giubellino,⁷ E. Gladysz-Dziadus,⁵¹ P. Glässel,³⁰ R. Gomez,^{104,77} E. G. Ferreira,³⁸ L. H. González-Trueba,²² P. González-Zamora,⁶² S. Gorbunov,²⁴ A. Goswami,¹⁰⁵ S. Gotovac,¹⁰⁶ L. K. Graczykowski,¹⁰³ R. Grajcarek,³⁰ A. Grelli,⁵⁹ A. Grigoras,⁷ C. Grigoras,⁷ V. Grigoriev,⁶⁴ A. Grigoryan,¹⁰⁷ S. Grigoryan,⁵² B. Grinyov,²¹ N. Grion,¹⁰¹ P. Gros,⁸⁵ J. F. Grosse-Oetringhaus,⁷ J.-Y. Grossiord,⁸⁴ R. Grosso,⁷ F. Guber,⁹⁹ R. Guernane,³⁷ B. Guerzoni,¹¹ M. Guilbaud,⁸⁴ K. Gulbrandsen,⁵⁴ H. Gulkanyan,¹⁰⁷ T. Gunji,¹⁰⁸ A. Gupta,⁴⁵ R. Gupta,⁴⁵ R. Haake,³¹ Ø. Haaland,²⁶ C. Hadjidakis,⁸⁸ M. Haiduc,⁹² H. Hamagaki,¹⁰⁸ G. Hamar,¹⁰ B. H. Han,¹⁰⁹ L. D. Hanratty,⁵⁰ A. Hansen,⁵⁴ Z. Harmanová-Tóthová,⁶⁶ J. W. Harris,⁵ M. Hartig,³⁶ A. Harton,¹⁰² D. Hatzifotiadou,¹⁹ S. Hayashi,¹⁰⁸ A. Hayrapetyan,^{7,107} S. T. Heckel,³⁶ M. Heide,³¹ H. Helstrup,²³ A. Herghelegiu,²⁸ G. Herrera Corral,⁷⁷ N. Herrmann,³⁰ B. A. Hess,¹¹⁰ K. F. Hetland,²³ B. Hicks,⁵ B. Hippolyte,⁵⁶ Y. Hori,¹⁰⁸ P. Hristov,⁷ I. Hřivnáčová,⁸⁸ M. Huang,²⁶ T. J. Humanic,³² D. S. Hwang,¹⁰⁹ R. Ichou,⁴³ R. Ilkaev,⁷² I. Ilkiv,⁹⁷ M. Inaba,⁶⁰ E. Incani,⁷⁹ P. G. Innocenti,⁷ G. M. Innocenti,¹⁵ M. Ippolitov,¹⁸ M. Irfan,¹³ C. Ivan,²⁹ M. Ivanov,²⁹ V. Ivanov,⁵⁸ A. Ivanov,²⁷ O. Ivanytskyi,²¹ A. Jacholkowski,⁴⁹ P. M. Jacobs,⁶⁹ C. Jahnke,⁷⁸ H. J. Jang,¹⁴ M. A. Janik,¹⁰³ P. H. S. Y. Jayarathna,⁵⁷ S. Jena,⁵⁵ D. M. Jha,⁶⁷ R. T. Jimenez Bustamante,⁹¹ P. G. Jones,⁵⁰ H. Jung,⁴⁴ A. Jusko,⁵⁰ A. B. Kaidalov,¹⁷ S. Kalcher,²⁴ P. Kaliňák,⁴⁷ T. Kalliokoski,⁴⁰ A. Kalweit,⁷ J. H. Kang,⁸¹ V. Kaplin,⁶⁴ S. Kar,¹² A. Karasu Uysal,^{7,111,112} O. Karavichev,⁹⁹ T. Karavicheva,⁹⁹ E. Karpechev,⁹⁹ A. Kazantsev,¹⁸ U. Kebschull,⁶³ R. Keidel,¹¹³ B. Ketzer,^{36,114} S. A. Khan,¹² M. M. Khan,¹³ P. Khan,⁸² K. H. Khan,¹⁶ A. Khanzadeev,⁵⁸ Y. Kharlov,⁶⁵ B. Kileng,²³ M. Kim,⁸¹ S. Kim,¹⁰⁹ M. Kim,⁴⁴ J. S. Kim,⁴⁴ J. H. Kim,¹⁰⁹ T. Kim,⁸¹ B. Kim,⁸¹ D. J. Kim,⁴⁰ D. W. Kim,^{44,14} S. Kirsch,²⁴ I. Kisel,²⁴ S. Kiselev,¹⁷ A. Kisiel,¹⁰³ J. L. Klay,¹¹⁵ J. Klein,³⁰ C. Klein-Bösing,³¹ M. Kliemant,³⁶ A. Kluge,⁷ M. L. Knichel,²⁹ A. G. Knospe,¹¹⁶ M. K. Köhler,²⁹ T. Kollegger,²⁴ A. Kolojvari,²⁷ M. Kompaniets,²⁷ V. Kondratiev,²⁷ N. Kondratyeva,⁶⁴ A. Konevskikh,⁹⁹ V. Kovalenko,²⁷ M. Kowalski,⁵¹ S. Kox,³⁷ G. Koyithatta Meethalevedu,⁵⁵ J. Kral,⁴⁰ I. Králik,⁴⁷ F. Kramer,³⁶ A. Kravčáková,⁶⁶ M. Krelina,³ M. Kretz,²⁴ M. Krivda,^{50,47} F. Krizek,⁴⁰ M. Krus,³ E. Kryshen,⁵⁸ M. Krzewicki,²⁹ V. Kucera,⁴ Y. Kucheriaev,¹⁸ T. Kugathasan,⁷ C. Kuhn,⁵⁶ P. G. Kuijper,⁶⁸ I. Kulakov,³⁶ J. Kumar,⁵⁵ P. Kurashvili,⁹⁷ A. Kurepin,⁹⁹ A. B. Kurepin,⁹⁹ A. Kuryakin,⁷² S. Kushpil,⁴ V. Kushpil,⁴ H. Kvaerno,⁵³ M. J. Kweon,³⁰ Y. Kwon,⁸¹ P. Ladrón de Guevara,⁹¹ I. Lakomov,⁸⁸ R. Langoy,^{26,117} S. L. La Pointe,⁵⁹ C. Lara,⁶³ A. Lardeux,³⁵ P. La Rocca,⁴⁹ R. Lea,⁷⁶ M. Lechman,⁷ S. C. Lee,⁴⁴ G. R. Lee,⁵⁰ I. Legrand,⁷ J. Lehnert,³⁶ R. C. Lemmon,¹¹⁸ M. Lenhardt,²⁹ V. Lenti,⁹⁶ H. León,²² M. Leoncino,¹⁵ I. León Monzón,¹⁰⁴ P. Lévai,¹⁰ S. Li,^{43,74} J. Lien,^{26,117} R. Lietava,⁵⁰ S. Lindal,⁵³ V. Lindenstruth,²⁴ C. Lippmann,^{29,7} M. A. Lisa,³² H. M. Ljunggren,⁸⁵ D. F. Lodato,⁵⁹ P. I. Loenne,²⁶ V. R. Loggins,⁶⁷ V. Loginov,⁶⁴ D. Lohner,³⁰ C. Loizides,⁶⁹ K. K. Loo,⁴⁰ X. Lopez,⁴³ E. López Torres,⁸⁰ G. Løvhøiden,⁵³ X.-G. Lu,³⁰ P. Luetig,³⁶ M. Lunardon,⁷³ J. Luo,⁷⁴ G. Luparello,⁵⁹ C. Luzzi,⁷ R. Ma,⁵ K. Ma,⁷⁴ D. M. Madagadhattige-Don,⁵⁷ A. Maevskaya,⁹⁹ M. Mager,^{119,7} D. P. Mahapatra,⁴⁸ A. Maire,³⁰ M. Malaev,⁵⁸ I. Maldonado Cervantes,⁹¹ L. Malinina,^{52,120} D. Mal'Kevich,¹⁷ P. Malzacher,²⁹ A. Mamonov,⁷² L. Manceau,⁸ L. Mangotra,⁴⁵ V. Manko,¹⁸ F. Manso,⁴³ N. Manukyan,¹⁰⁷ V. Manzari,⁹⁶ Y. Mao,⁷⁴ M. Marchisone,^{43,15} J. Mareš,¹²¹ G. V. Margagliotti,^{76,101} A. Margotti,¹⁹ A. Marín,²⁹ C. Markert,¹¹⁶ M. Marquard,³⁶ I. Martashvili,¹²² N. A. Martin,²⁹ P. Martinengo,⁷ M. I. Martínez,⁹⁰ A. Martínez Davalos,²² G. Martínez García,³⁵ Y. Martynov,²¹ A. Mas,³⁵ S. Masciocchi,²⁹ M. Maserà,¹⁵ A. Masoni,⁸⁷ L. Massacrier,³⁵ A. Mastroserio,²⁵ A. Matyja,⁵¹ C. Mayer,⁵¹ J. Mazer,¹²² M. A. Mazzoni,⁹⁸ F. Meddi,¹²³ A. Menchaca-Rocha,²² J. Mercado Pérez,³⁰ M. Meres,⁷¹ Y. Miake,⁶⁰ K. Mikhaylov,^{52,17} L. Milano,^{7,15} J. Milosevic,^{53,124} A. Mischke,⁵⁹ A. N. Mishra,^{105,125} D. Miśkowiec,²⁹ C. Mitu,⁹² S. Mizuno,⁶⁰ J. Mlynarz,⁶⁷ B. Mohanty,^{12,126} L. Molnar,^{10,56} L. Montaña Zetina,⁷⁷ M. Monteno,⁸ E. Montes,⁶² T. Moon,⁸¹ M. Morando,⁷³ D. A. Moreira De Godoy,⁷⁸ S. Moretto,⁷³ A. Morreale,⁴⁰ A. Morsch,⁷ V. Muccifora,⁶¹ E. Mudnic,¹⁰⁶ S. Muhuri,¹² M. Mukherjee,¹² H. Müller,⁷ M. G. Munhoz,⁷⁸ S. Murray,⁴¹ L. Musa,⁷ J. Musinsky,⁴⁷ B. K. Nandi,⁵⁵ R. Nania,¹⁹ E. Nappi,⁹⁶ C. Nattrass,¹²² T. K. Nayak,¹² S. Nazarenko,⁷² A. Nedosekin,¹⁷ M. Nicassio,^{25,29} M. Niculescu,^{92,7} B. S. Nielsen,⁵⁴ T. Niida,⁶⁰ S. Nikolaev,¹⁸ V. Nikolic,³³ S. Nikulin,¹⁸ V. Nikulin,⁵⁸ B. S. Nilsen,⁸³ M. S. Nilsson,⁵³ F. Noferini,^{19,20} P. Nomokonov,⁵² G. Nooren,⁵⁹ A. Nyanin,¹⁸ A. Nyatha,⁵⁵ C. Nygaard,⁵⁴ J. Nystrand,²⁶ A. Ochirov,⁸ H. Oeschler,^{119,7,30} S. Oh,⁵ S. K. Oh,⁴⁴ J. Oleniacz,¹⁰³ A. C. Oliveira Da Silva,⁷⁸ C. Oppedisano,⁸ A. Ortiz Velasquez,^{85,91} A. Oskarsson,⁸⁵ P. Ostrowski,¹⁰³ J. Otwinowski,²⁹ K. Oyama,³⁰ K. Ozawa,¹⁰⁸

Y. Pachmayer,³⁰ M. Pachr,³ F. Padilla,¹⁵ P. Pagano,⁹⁵ G. Pačić,⁹¹ F. Painke,²⁴ C. Pajares,³⁸ S. K. Pal,¹² A. Palaha,⁵⁰ A. Palmeri,⁴² V. Papikyan,¹⁰⁷ G. S. Pappalardo,⁴² W. J. Park,²⁹ A. Passfeld,³¹ D. I. Patalakha,⁶⁵ V. Paticchio,⁹⁶ B. Paul,⁸² A. Pavlinov,⁶⁷ T. Pawlak,¹⁰³ T. Peitzmann,⁵⁹ H. Pereira Da Costa,⁴⁶ E. Pereira De Oliveira Filho,⁷⁸ D. Peresunko,¹⁸ C. E. Pérez Lara,⁶⁸ D. Perrino,²⁵ W. Peryt,¹⁰³ A. Pesci,¹⁹ Y. Pestov,¹²⁷ V. Petráček,³ M. Petran,³ M. Petris,²⁸ P. Petrov,⁵⁰ M. Petrovici,²⁸ C. Petta,⁴⁹ S. Piano,¹⁰¹ M. Pikna,⁷¹ P. Pillot,³⁵ O. Pinazza,⁷ L. Pinsky,⁵⁷ N. Pitz,³⁶ D. B. Piyarathna,⁵⁷ M. Planinic,³³ M. Płoskoń,⁶⁹ J. Pluta,¹⁰³ T. Pocheptsov,⁵² S. Pochybova,¹⁰ P. L. M. Podesta-Lerma,¹⁰⁴ M. G. Poghosyan,⁷ K. Polák,¹²¹ B. Polichtchouk,⁶⁵ N. Poljak,^{59,33} A. Pop,²⁸ S. Porteboeuf-Houssais,⁴³ V. Pospíšil,³ B. Potukuchi,⁴⁵ S. K. Prasad,⁶⁷ R. Preghenella,^{19,20} F. Prino,⁸ C. A. Pruneau,⁶⁷ I. Pshenichnov,⁹⁹ G. Puddu,⁷⁹ V. Punin,⁷² M. Putiš,⁶⁶ J. Putschke,⁶⁷ H. Qvigstad,⁵³ A. Rachevski,¹⁰¹ A. Rademakers,⁷ T. S. Rähä,⁴⁰ J. Rak,⁴⁰ A. Rakotozafindrabe,⁴⁶ L. Ramello,⁸⁹ S. Raniwala,¹⁰⁵ R. Raniwala,¹⁰⁵ S. S. Räsänen,⁴⁰ B. T. Ranganu,³⁶ D. Rathee,⁶ W. Rauch,⁷ K. F. Read,¹²² J. S. Real,³⁷ K. Redlich,^{97,128} R. J. Reed,⁵ A. Rehman,²⁶ P. Reichelt,³⁶ M. Reicher,⁵⁹ R. Renfordt,³⁶ A. R. Reolon,⁶¹ A. Reshetin,⁹⁹ F. Rettig,²⁴ J.-P. Revol,⁷ K. Reygers,³⁰ L. Riccati,⁸ R. A. Ricci,¹²⁹ T. Richert,⁸⁵ M. Richter,⁵³ P. Riedler,⁷ W. Riegler,⁷ F. Riggi,^{49,42} M. Rodríguez Cahuantzi,⁹⁰ A. Rodriguez Manso,⁶⁸ K. Røed,^{26,53} E. Rogochaya,⁵² D. Rohr,²⁴ D. Röhrich,²⁶ R. Romita,^{29,118} F. Ronchetti,⁶¹ P. Rosnet,⁴³ S. Rossegger,⁷ A. Rossi,^{7,73} P. Roy,⁸² C. Roy,⁵⁶ A. J. Rubio Montero,⁶² R. Rui,⁷⁶ R. Russo,¹⁵ E. Ryabinkin,¹⁸ A. Rybicki,⁵¹ S. Sadovsky,⁶⁵ K. Šafařík,⁷ R. Sahoo,¹²⁵ P. K. Sahu,⁴⁸ J. Saini,¹² H. Sakaguchi,¹³⁰ S. Sakai,⁶⁹ D. Sakata,⁶⁰ C. A. Salgado,³⁸ J. Salzwedel,³² S. Sambyal,⁴⁵ V. Samsonov,⁵⁸ X. Sanchez Castro,⁵⁶ L. Šándor,⁴⁷ A. Sandoval,²² M. Sano,⁶⁰ G. Santagati,⁴⁹ R. Santoro,^{7,20} J. Sarkamo,⁴⁰ D. Sarkar,¹² E. Scapparone,¹⁹ F. Scarlassara,⁷³ R. P. Scharenberg,⁷⁰ C. Schiaua,²⁸ R. Schicker,³⁰ H. R. Schmidt,¹¹⁰ C. Schmidt,²⁹ S. Schuchmann,³⁶ J. Schukraft,⁷ T. Schuster,⁵ Y. Schutz,^{7,35} K. Schwarz,²⁹ K. Schweda,²⁹ G. Scioli,¹¹ E. Scomparin,⁸ R. Scott,¹²² P. A. Scott,⁵⁰ G. Segato,⁷³ I. Selyuzhenkov,²⁹ S. Senyukov,⁵⁶ J. Seo,⁸⁶ S. Serchi,⁷⁹ E. Serradilla,^{62,22} A. Sevcenco,⁹² A. Shabetai,³⁵ G. Shabratova,⁵² R. Shahoyan,⁷ N. Sharma,¹²² S. Sharma,⁴⁵ S. Rohni,⁴⁵ K. Shigaki,¹³⁰ K. Shtejer,⁸⁰ Y. Sibiriyak,¹⁸ E. Sickling,³¹ S. Siddhanta,⁸⁷ T. Siemiarczuk,⁹⁷ D. Silvermyr,³⁹ C. Silvestre,³⁷ G. Simatovic,^{91,33} G. Simonetti,⁷ R. Singaraju,¹² R. Singh,⁴⁵ S. Singha,^{12,126} V. Singhal,¹² B. C. Sinha,¹² T. Sinha,⁸² B. Sitar,⁷¹ M. Sitta,⁸⁹ T. B. Skaali,⁵³ K. Skjerdal,²⁶ R. Smakal,³ N. Smirnov,⁵ R. J. M. Snellings,⁵⁹ C. Sjøgaard,⁸⁵ R. Soltz,² M. Song,⁸¹ J. Song,⁸⁶ C. Soos,⁷ F. Soramel,⁷³ I. Sputowska,⁵¹ M. Spyropoulou-Stassinaki,¹⁰⁰ B. K. Srivastava,⁷⁰ J. Stachel,³⁰ I. Stan,⁹² G. Stefanek,⁹⁷ M. Steinpreis,³² E. Stenlund,⁸⁵ G. Steyn,⁴¹ J. H. Stiller,³⁰ D. Stocco,³⁵ M. Stolpovskiy,⁶⁵ P. Strmen,⁷¹ A. A. P. Suaide,⁷⁸ M. A. Subieta Vásquez,¹⁵ T. Sugitate,¹³⁰ C. Suire,⁸⁸ R. Sultanov,¹⁷ M. Šumbera,⁴ T. Susa,³³ T. J. M. Symons,⁶⁹ A. Szanto de Toledo,⁷⁸ I. Szarka,⁷¹ A. Szczepankiewicz,^{51,7} M. Szymański,¹⁰³ J. Takahashi,⁹⁴ M. A. Tangaro,²⁵ J. D. Tapia Takaki,⁸⁸ A. Tarantola Peloni,³⁶ A. Tarazona Martinez,⁷ A. Tauro,⁷ G. Tejada Muñoz,⁹⁰ A. Telesca,⁷ A. Ter Minasyan,¹⁸ C. Terrevoli,²⁵ J. Thäder,²⁹ D. Thomas,⁵⁹ R. Tieulent,⁸⁴ A. R. Timmins,⁵⁷ D. Tlusty,³ A. Toia,^{24,73,34} H. Torii,¹⁰⁸ L. Toscano,⁸ V. Trubnikov,²¹ D. Truesdale,³² W. H. Trzaska,⁴⁰ T. Tsuji,¹⁰⁸ A. Tumkin,⁷² R. Turrisi,³⁴ T. S. Tveter,⁵³ J. Ulery,³⁶ K. Ullaland,²⁶ J. Ulrich,^{131,63} A. Uras,⁸⁴ G. M. Urciuoli,⁹⁸ G. L. Usai,⁷⁹ M. Vajzer,^{3,4} M. Vala,^{52,47} L. Valencia Palomo,⁸⁸ P. Vande Vyvre,⁷ J. W. Van Hoorne,⁷ M. van Leeuwen,⁵⁹ L. Vannucci,¹²⁹ A. Vargas,⁹⁰ R. Varma,⁵⁵ M. Vasileiou,¹⁰⁰ A. Vasiliev,¹⁸ V. Vechernin,²⁷ M. Veldhoen,⁵⁹ M. Venaruzzo,⁷⁶ E. Vercellin,¹⁵ S. Vergara,⁹⁰ R. Vernet,¹³² M. Verweij,⁵⁹ L. Vickovic,¹⁰⁶ G. Viesti,⁷³ J. Viinikainen,⁴⁰ Z. Vilakazi,⁴¹ O. Villalobos Baillie,⁵⁰ Y. Vinogradov,⁷² L. Vinogradov,²⁷ A. Vinogradov,¹⁸ T. Virgili,⁹⁵ Y. P. Viyogi,¹² A. Vodopyanov,⁵² M. A. Völkl,³⁰ S. Voloshin,⁶⁷ K. Voloshin,¹⁷ G. Volpe,⁷ B. von Haller,⁷ I. Vorobyev,²⁷ D. Vranic,^{29,7} J. Vrláková,⁶⁶ B. Vulpescu,⁴³ A. Vyushin,⁷² B. Wagner,²⁶ V. Wagner,³ R. Wan,⁷⁴ Y. Wang,⁷⁴ M. Wang,⁷⁴ Y. Wang,³⁰ K. Watanabe,⁶⁰ M. Weber,⁵⁷ J. P. Wessels,^{7,31} U. Westerhoff,³¹ J. Wiechula,¹¹⁰ J. Wikne,⁵³ M. Wilde,³¹ G. Wilk,⁹⁷ M. C. S. Williams,¹⁹ B. Windelband,³⁰ L. Xaplanteris Karampatsos,¹¹⁶ C. G. Yaldo,⁶⁷ Y. Yamaguchi,¹⁰⁸ S. Yang,²⁶ P. Yang,⁷⁴ H. Yang,^{46,59} S. Yasnopolskiy,¹⁸ J. Yi,⁸⁶ Z. Yin,⁷⁴ I.-K. Yoo,⁸⁶ J. Yoon,⁸¹ W. Yu,³⁶ X. Yuan,⁷⁴ I. Yushmanov,¹⁸ V. Zaccolo,⁵⁴ C. Zach,³ C. Zampolli,¹⁹ S. Zaporozhets,⁵² A. Zarochentsev,²⁷ P. Závada,¹²¹ N. Zaviyalov,⁷² H. Zbroszczyk,¹⁰³ P. Zelnicsek,⁶³ I. S. Zgura,⁹² M. Zhalov,⁵⁸ H. Zhang,⁷⁴ X. Zhang,^{69,43,74} Y. Zhang,⁷⁴ D. Zhou,⁷⁴ F. Zhou,⁷⁴ Y. Zhou,⁵⁹ H. Zhu,⁷⁴ J. Zhu,⁷⁴ X. Zhu,⁷⁴ J. Zhu,⁷⁴ A. Zichichi,^{11,20} A. Zimmermann,³⁰ G. Zinovjev,²¹ Y. Zoccarato,⁸⁴ M. Zynovjev,²¹ and M. Zyzak³⁶

(ALICE Collaboration)

- ¹Academy of Scientific Research and Technology (ASRT), Cairo, Egypt
²Lawrence Livermore National Laboratory, Livermore, California, USA
³Faculty of Nuclear Sciences and Physical Engineering, Czech Technical University in Prague, Prague, Czech Republic
⁴Nuclear Physics Institute, Academy of Sciences of the Czech Republic, Řež u Prahy, Czech Republic
⁵Yale University, New Haven, Connecticut, USA
⁶Physics Department, Panjab University, Chandigarh, India
⁷European Organization for Nuclear Research (CERN), Geneva, Switzerland
⁸Sezione INFN, Turin, Italy
⁹Politecnico di Torino, Turin, Italy
¹⁰Wigner Research Centre for Physics, Hungarian Academy of Sciences, Budapest, Hungary
¹¹Dipartimento di Fisica e Astronomia dell'Università and Sezione INFN, Bologna, Italy
¹²Variable Energy Cyclotron Centre, Kolkata, India
¹³Department of Physics, Aligarh Muslim University, Aligarh, India
¹⁴Korea Institute of Science and Technology Information, Daejeon, South Korea
¹⁵Dipartimento di Fisica dell'Università and Sezione INFN, Turin, Italy
¹⁶COMSATS Institute of Information Technology (CIIT), Islamabad, Pakistan
¹⁷Institute for Theoretical and Experimental Physics, Moscow, Russia
¹⁸Russian Research Centre Kurchatov Institute, Moscow, Russia
¹⁹Sezione INFN, Bologna, Italy
²⁰Centro Fermi-Museo Storico della Fisica e Centro Studi e Ricerche "Enrico Fermi," Rome, Italy
²¹Bogolyubov Institute for Theoretical Physics, Kiev, Ukraine
²²Instituto de Física, Universidad Nacional Autónoma de México, Mexico City, Mexico
²³Faculty of Engineering, Bergen University College, Bergen, Norway
²⁴Frankfurt Institute for Advanced Studies, Johann Wolfgang Goethe-Universität Frankfurt, Frankfurt, Germany
²⁵Dipartimento Interateneo di Fisica "M. Merlin" and Sezione INFN, Bari, Italy
²⁶Department of Physics and Technology, University of Bergen, Bergen, Norway
²⁷V. Fock Institute for Physics, St. Petersburg State University, St. Petersburg, Russia
²⁸National Institute for Physics and Nuclear Engineering, Bucharest, Romania
²⁹Research Division and ExtreMe Matter Institute EMMI, GSI Helmholtzzentrum für Schwerionenforschung, Darmstadt, Germany
³⁰Physikalisches Institut, Ruprecht-Karls-Universität Heidelberg, Heidelberg, Germany
³¹Institut für Kernphysik, Westfälische Wilhelms-Universität Münster, Münster, Germany
³²Department of Physics, The Ohio State University, Columbus, Ohio, USA
³³Rudjer Bošković Institute, Zagreb, Croatia
³⁴Sezione INFN, Padova, Italy
³⁵SUBATECH, Ecole des Mines de Nantes, Université de Nantes, CNRS-IN2P3, Nantes, France
³⁶Institut für Kernphysik, Johann Wolfgang Goethe-Universität Frankfurt, Frankfurt, Germany
³⁷Laboratoire de Physique Subatomique et de Cosmologie (LPSC), Université Joseph Fourier, CNRS-IN2P3, Institut Polytechnique de Grenoble, Grenoble, France
³⁸Departamento de Física de Partículas and IGFAE, Universidad de Santiago de Compostela, Santiago de Compostela, Spain
³⁹Oak Ridge National Laboratory, Oak Ridge, Tennessee, USA
⁴⁰Helsinki Institute of Physics (HIP) and University of Jyväskylä, Jyväskylä, Finland
⁴¹Physics Department, University of Cape Town and iThemba LABS, National Research Foundation, Somerset West, South Africa
⁴²Sezione INFN, Catania, Italy
⁴³Laboratoire de Physique Corpusculaire (LPC), Clermont Université, Université Blaise Pascal, CNRS-IN2P3, Clermont-Ferrand, France
⁴⁴Gangneung-Wonju National University, Gangneung, South Korea
⁴⁵Physics Department, University of Jammu, Jammu, India
⁴⁶Commissariat à l'Energie Atomique, IRFU, Saclay, France
⁴⁷Institute of Experimental Physics, Slovak Academy of Sciences, Košice, Slovakia
⁴⁸Institute of Physics, Bhubaneswar, India
⁴⁹Dipartimento di Fisica e Astronomia dell'Università and Sezione INFN, Catania, Italy
⁵⁰School of Physics and Astronomy, University of Birmingham, Birmingham, United Kingdom
⁵¹The Henryk Niewodniczanski Institute of Nuclear Physics, Polish Academy of Sciences, Cracow, Poland
⁵²Joint Institute for Nuclear Research (JINR), Dubna, Russia
⁵³Department of Physics, University of Oslo, Oslo, Norway
⁵⁴Niels Bohr Institute, University of Copenhagen, Copenhagen, Denmark
⁵⁵Indian Institute of Technology Bombay (IIT), Mumbai, India
⁵⁶Institut Pluridisciplinaire Hubert Curien (IPHC), Université de Strasbourg, CNRS-IN2P3, Strasbourg, France
⁵⁷University of Houston, Houston, Texas, USA
⁵⁸Petersburg Nuclear Physics Institute, Gatchina, Russia
⁵⁹Nikhef, National Institute for Subatomic Physics and Institute for Subatomic Physics of Utrecht University, Utrecht, Netherlands

- ⁶⁰University of Tsukuba, Tsukuba, Japan
- ⁶¹Laboratori Nazionali di Frascati, INFN, Frascati, Italy
- ⁶²Centro de Investigaciones Energéticas Medioambientales y Tecnológicas (CIEMAT), Madrid, Spain
- ⁶³Institut für Informatik, Johann Wolfgang Goethe-Universität Frankfurt, Frankfurt, Germany
- ⁶⁴Moscow Engineering Physics Institute, Moscow, Russia
- ⁶⁵Institute for High Energy Physics, Protvino, Russia
- ⁶⁶Faculty of Science, P.J. Šafárik University, Košice, Slovakia
- ⁶⁷Wayne State University, Detroit, Michigan, USA
- ⁶⁸Nikhef, National Institute for Subatomic Physics, Amsterdam, Netherlands
- ⁶⁹Lawrence Berkeley National Laboratory, Berkeley, California, USA
- ⁷⁰Purdue University, West Lafayette, Indiana, USA
- ⁷¹Faculty of Mathematics, Physics and Informatics, Comenius University, Bratislava, Slovakia
- ⁷²Russian Federal Nuclear Center (VNIIEF), Sarov, Russia
- ⁷³Dipartimento di Fisica e Astronomia dell'Università and Sezione INFN, Padova, Italy
- ⁷⁴Central China Normal University, Wuhan, China
- ⁷⁵Sección Física, Departamento de Ciencias, Pontificia Universidad Católica del Perú, Lima, Peru
- ⁷⁶Dipartimento di Fisica dell'Università and Sezione INFN, Trieste, Italy
- ⁷⁷Centro de Investigación y de Estudios Avanzados (CINVESTAV), Mexico City and Mérida, Mexico
- ⁷⁸Universidade de São Paulo (USP), São Paulo, Brazil
- ⁷⁹Dipartimento di Fisica dell'Università and Sezione INFN, Cagliari, Italy
- ⁸⁰Centro de Aplicaciones Tecnológicas y Desarrollo Nuclear (CEADEN), Havana, Cuba
- ⁸¹Yonsei University, Seoul, South Korea
- ⁸²Saha Institute of Nuclear Physics, Kolkata, India
- ⁸³Physics Department, Creighton University, Omaha, Nebraska, USA
- ⁸⁴Université de Lyon, Université Lyon 1, CNRS/IN2P3, IPN-Lyon, Villeurbanne, France
- ⁸⁵Division of Experimental High Energy Physics, University of Lund, Lund, Sweden
- ⁸⁶Pusan National University, Pusan, South Korea
- ⁸⁷Sezione INFN, Cagliari, Italy
- ⁸⁸Institut de Physique Nucléaire d'Orsay (IPNO), Université Paris-Sud, CNRS-IN2P3, Orsay, France
- ⁸⁹Dipartimento di Scienze e Innovazione Tecnologica dell'Università del Piemonte Orientale and Gruppo Collegato INFN, Alessandria, Italy
- ⁹⁰Benemérita Universidad Autónoma de Puebla, Puebla, Mexico
- ⁹¹Instituto de Ciencias Nucleares, Universidad Nacional Autónoma de México, Mexico City, Mexico
- ⁹²Institute of Space Sciences (ISS), Bucharest, Romania
- ⁹³Bose Institute, Department of Physics and Centre for Astroparticle Physics and Space Science (CAPSS), Kolkata, India
- ⁹⁴Universidade Estadual de Campinas (UNICAMP), Campinas, Brazil
- ⁹⁵Dipartimento di Fisica "E.R. Caianiello" dell'Università and Gruppo Collegato INFN, Salerno, Italy
- ⁹⁶Sezione INFN, Bari, Italy
- ⁹⁷National Centre for Nuclear Studies, Warsaw, Poland
- ⁹⁸Sezione INFN, Rome, Italy
- ⁹⁹Institute for Nuclear Research, Academy of Sciences, Moscow, Russia
- ¹⁰⁰Physics Department, University of Athens, Athens, Greece
- ¹⁰¹Sezione INFN, Trieste, Italy
- ¹⁰²Chicago State University, Chicago, Illinois, USA
- ¹⁰³Warsaw University of Technology, Warsaw, Poland
- ¹⁰⁴Universidad Autónoma de Sinaloa, Culiacán, Mexico
- ¹⁰⁵Physics Department, University of Rajasthan, Jaipur, India
- ¹⁰⁶Technical University of Split FESB, Split, Croatia
- ¹⁰⁷A. I. Alikhanyan National Science Laboratory (Yerevan Physics Institute) Foundation, Yerevan, Armenia
- ¹⁰⁸University of Tokyo, Tokyo, Japan
- ¹⁰⁹Department of Physics, Sejong University, Seoul, South Korea
- ¹¹⁰Eberhard Karls Universität Tübingen, Tübingen, Germany
- ¹¹¹Yildiz Technical University, Istanbul, Turkey
- ¹¹²KTO Karatay University, Konya, Turkey
- ¹¹³Zentrum für Technologietransfer und Telekommunikation (ZTT), Fachhochschule Worms, Worms, Germany
- ¹¹⁴Technische Universität München, Munich, Germany
- ¹¹⁵California Polytechnic State University, San Luis Obispo, California, USA
- ¹¹⁶The University of Texas at Austin, Physics Department, Austin, Texas, USA
- ¹¹⁷Vestfold University College, Tonsberg, Norway
- ¹¹⁸Nuclear Physics Group, STFC Daresbury Laboratory, Daresbury, United Kingdom
- ¹¹⁹Institut für Kernphysik, Technische Universität Darmstadt, Darmstadt, Germany

- ¹²⁰*M.V. Lomonosov Moscow State University, D.V. Skobeltsyn Institute of Nuclear Physics, Moscow, Russia*
¹²¹*Institute of Physics, Academy of Sciences of the Czech Republic, Prague, Czech Republic*
¹²²*University of Tennessee, Knoxville, Tennessee, USA*
¹²³*Dipartimento di Fisica dell'Università "La Sapienza" and Sezione INFN, Rome, Italy*
¹²⁴*University of Belgrade, Faculty of Physics and "Vina" Institute of Nuclear Sciences, Belgrade, Serbia*
¹²⁵*Indian Institute of Technology Indore (IIT), Indore, India*
¹²⁶*National Institute of Science Education and Research, Bhubaneswar, India*
¹²⁷*Budker Institute for Nuclear Physics, Novosibirsk, Russia*
¹²⁸*Institut of Theoretical Physics, University of Wroclaw, Wroclaw, Poland*
¹²⁹*Laboratori Nazionali di Legnaro, INFN, Legnaro, Italy*
¹³⁰*Hiroshima University, Hiroshima, Japan*
¹³¹*Kirchhoff-Institut für Physik, Ruprecht-Karls-Universität Heidelberg, Heidelberg, Germany*
¹³²*Centre de Calcul de l'IN2P3, Villeurbanne, France*